ORAL/POSTER REFERENCE: ICF100373OR

CRACK VELOCITY DEPENDENT TOUGHNESS IN RATE DEPENDENT MATERIALS

Chad M. Landis[1], Thomas Pardoen[2] and John W. Hutchinson[3]

[1]MEMS, MS 321, Rice University, PO Box 1892, Houston, TX 77251
[2]Département des Sciences des Matériaux et des Procédés, Université catholique de Louvain, PCIM, Lovain-la-Neuve, Belgium
[3]DEAS, Harvard University, Cambridge, MA 02138

ABSTRACT

Mode I, quasi-static, steady state crack growth is analyzed for rate dependent materials under plane strain conditions in small scale yielding. The solid is characterized by an elastic-viscoplastic constitutive law and the plane ahead of the crack tip is embedded with a rate dependent fracture process zone. The macroscopic work of fracture of the material is computed as a function of the crack velocity and the parameters characterizing the fracture process zone and the solid. With increasing crack velocity a competition exists between the strain rate hardening of the solid, which causes elevated tractions ahead of the crack tip that tend to drive crack propagation, and the rate strengthening of the fracture process zone which tends to resist fracture. Results for material parameters characteristic of polymers show that the toughness of the material can either increase or decrease with increasing crack velocity. To motivate the model, the cohesive zone parameters are discussed in terms of failure mechanisms such as crazing and void growth ahead of the crack tip. The toughness of rubber modified epoxies is explained by employing the fracture model along with micromechanical void cell calculations.

KEYWORDS

Steady state fracture, elastic-viscoplastic material, cohesive zone model

1. INTRODUCTION

In this work the toughness of a rate dependent material is determined as a function of certain intrinsic material properties. An elastic-viscoplastic constitutive law characterizes the bulk material deformation and a rate dependent cohesive zone law describes the separation ahead of the crack tip. A steady state finite element formulation, Dean and Hutchinson [1], is used to determine the stress and strain fields around the moving crack and to relate the critical applied energy release rate to the intrinsic material toughness.

Figure 1 is a schematic of a crack propagating in an elastic-plastic solid under Mode I, plane strain, small scale yielding, steady state conditions. The displayed shape of the plastic zone is the result of a calculation for an elastic-perfectly plastic, rate independent material. The plastic zone shape for rate dependent materials is similar in both size and shape. Far from the crack tip the stresses follow the Mode I elastic *K* field. As the crack propagates through the solid the crack tip is surrounded by active plasticity, elastic unloading and plastic reloading sectors, Drugan *et al*. [2]. Far behind the crack tip there is a wake of residual plastic strains where the material has unloaded elastically.

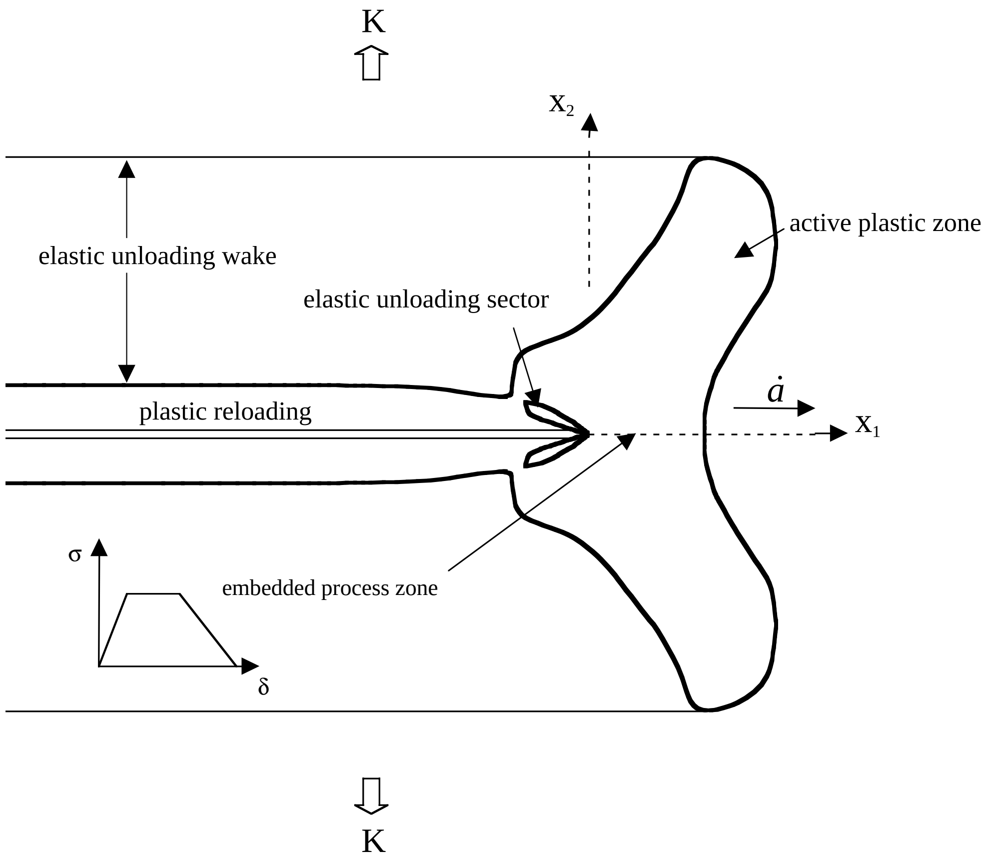

Figure 1: The plastic zone near a steadily propagating crack in an elastic-perfectly plastic material.

2. GOVERNING EQUATIONS

We adopt a rate dependent elastic-viscoplastic constitutive model of the form used by Marusich and Ortiz [3] and Xia and Shih [4],

$$\left(1+\frac{\dot{\bar{\varepsilon}}^{p}}{\dot{\varepsilon}_{o}}\right)=\left(\frac{\bar{\sigma}}{\sigma_{y}}\right)^{m}, \; if \;\; \bar{\sigma} \geq \sigma_{y} \tag{1}$$

$$\dot{\bar{\varepsilon}}^{p}=0, \text{ if } \bar{\sigma}<\sigma_{y} \tag{2}$$

where $\bar{\sigma} = \sqrt{\frac{3}{2} s_{ij} s_{ij}}$ is the effective stress, $s_{ij} = \sigma_{ij} - \frac{1}{3}\sigma_{kk}\delta_{ij}$ is the deviatoric stress tensor, σ_y is the static tensile yield strength, $\dot{\bar{\varepsilon}}^p = \sqrt{\frac{2}{3}\dot{\varepsilon}_{ij}^p \dot{\varepsilon}_{ij}^p}$ is the effective plastic strain rate, $\dot{\varepsilon}_o$ is a reference plastic strain rate and m is the plastic strain rate sensitivity exponent.

The components of the plastic strain rate are then given by

$$\dot{\varepsilon}_{ij}^p = \frac{3}{2}\dot{\bar{\varepsilon}}^p \frac{s_{ij}}{\bar{\sigma}} \tag{3}$$

Finally, the elastic strain rates are given by

$$\dot{\varepsilon}_{ij}^e = \frac{1+\nu}{E}\dot{\sigma}_{ij} - \frac{\nu}{E}\dot{\sigma}_{kk}\delta_{ij} \tag{4}$$

where E and ν are the isotropic Young's modulus and Poisson's ratio. Notice that this form of the constitutive law allows for a well-defined region of elastic response which is required for the small scale yielding approximation to be used.

The rate dependence for the fracture process zone is taken to follow a similar functional form as that for the bulk solid. In order to facilitate the finite element calculations it is assumed that there is always an initial linear portion in the traction-separation law. Hence, the crack opening displacement, δ, is the sum of an elastic (linear) and a plastic part. The cohesive traction obeys

$$\dot{t} = \hat{\sigma}\lambda_1 \frac{\left(\dot{\delta} - \dot{\delta}^p\right)}{\delta_c} \tag{5}$$

where λ_1 is a shape parameter of the static traction-opening law (see Tvergaard and Hutchinson [5]), $\hat{\sigma}$ is the peak stress of the static form of the traction-separation law and δ_c is the critical crack opening where tractions drop to zero. The second shape parameter of the traction-separation law is λ_2. The plastic opening rate, $\dot{\delta}^p$, is described by

$$\left(1 + \frac{\dot{\delta}^p}{\dot{\delta}_o}\right) = \left(\frac{t}{t_o\left(\delta^p\right)}\right)^q \text{ for } t > t_o\left(\delta^p\right) \tag{6}$$

$$\dot{\delta}^p = 0 \text{ for } t < t_o\left(\delta^p\right) \tag{7}$$

$$t = 0 \text{ if } \delta > \delta_c \tag{8}$$

where $\dot{\delta}_o$ is a characteristic crack opening rate, t is the normal traction acting on the crack plane, q is the rate exponent of the fracture process zone and $t_o\left(\delta^p\right)$ represents the static form of the traction-separation law. We also impose the condition (8) requiring that the total crack opening, δ, must always be less than the critical crack opening, δ_c, for all applied opening rates otherwise the traction must drop to zero. A more detailed description of the traction-separation law can be found in Landis *et al*. [6].

3. RESULTS

Dimensional analysis suggests that the macroscopic steady state toughness depends on the following dimensionless parameters

$$\frac{\Gamma_{ss}}{\Gamma_o} = \overline{\Gamma}\left(\frac{\dot{a}}{R_o \dot{\varepsilon}_o}, \frac{\hat{\sigma}}{\sigma_y}, \frac{\dot{\delta}_o}{\delta_c \dot{\varepsilon}_o}, m, q, \frac{\sigma_y}{E}, \nu, \lambda_1, \lambda_2 \right) \tag{9}$$

where $\dot{a}$ is the crack velocity and

$$R_o = \frac{1}{3\pi}\left(\frac{E}{1-\nu^2}\right)\frac{\Gamma_o}{\sigma_y^2} = \frac{1}{3\pi}\left(\frac{K_o}{\sigma_y}\right)^2 \tag{10}$$

is the approximate size of the plastic zone when the applied energy release rate, K, is equal to K_o, where K_o is related to Γ_o through (10). Previous studies on rate independent materials have demonstrated that the last 4 parameters in (9) are of secondary importance. For this study the parameters $E/\sigma_y = 50$, $\nu = 0.35$, $\lambda_1 = 0.15$ and $\lambda_2 = 0.5$ are used.

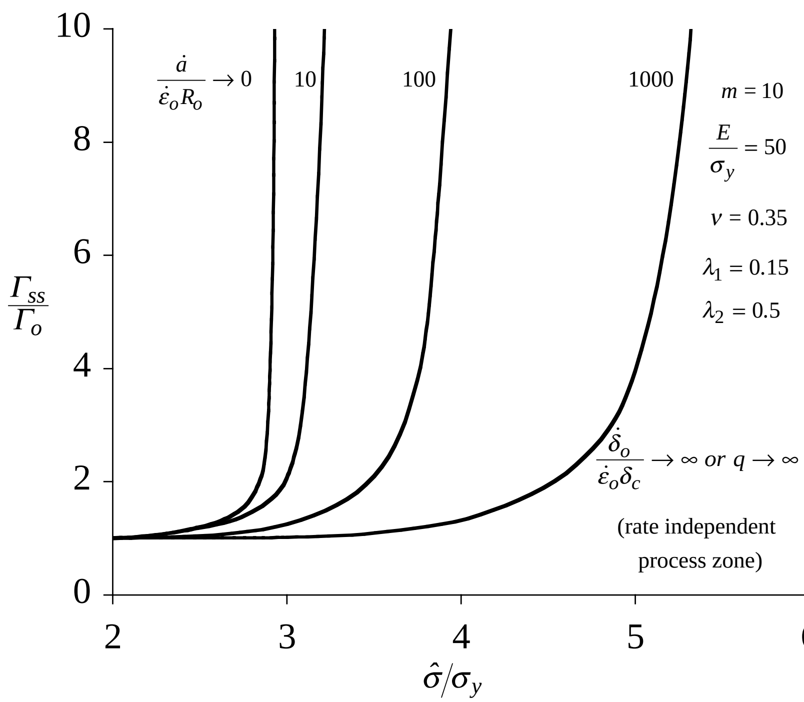

Figure 2: Steady state toughness versus peak cohesive strength for a rate independent cohesive zone law.

The first set of results shown in Figure 2 are for a solid with rate exponent $m = 10$ and a rate independent fracture process zone. The rate independent fracture process zone is a limiting case of Equations (6-8) with $\dot{\delta}_o/(\dot{\varepsilon}_o \delta_c) \to \infty$ or $q \to \infty$. Figure 2 plots the steady state toughness as a function of the peak cohesive stress in the fracture process zone. For values of $\hat{\sigma} < 2\sigma_y$ the plasticity in the bulk solid is not of sufficient intensity to induce a significant amount of dissipation and the steady state toughness is only slightly greater than Γ_o. For exceedingly slow crack velocities the model reduces to a rate-independent elastic-perfectly plastic material where the solid cannot sustain normal tractions greater than approximately $2.96\sigma_y$ ahead of the crack tip. Hence, if $\hat{\sigma} > 2.96\sigma_y$ then the fracture process zone cannot separate and Γ_{ss} is infinite. At finite crack velocities the strain rate effects in the solid become relevant. Increasing crack velocities allow for elevated normal traction acting on the crack plane. However, the normal traction ahead of the crack tip cannot exceed $\hat{\sigma}$ which limits the intensity of the plastic deformation and hence the toughness of the material decreases as crack velocity increases. The effects shown in Figure 2 are analogous to strain hardening or strain gradient hardening effects in rate independent materials, Wei and Hutchinson [7]. The general trend is that material hardening elevates tractions ahead of the crack tip which promote the separation of the fracture process zone.

The introduction of a rate dependent fracture process zone sets up a competition between the hardening of the solid and the strengthening of the cohesive zone. As such, trends in the steady state toughness are not as straightforward as those for the rate independent fracture process. Furthermore, Γ_{ss} is sensitive to the two rate parameters associated with the fracture process, q and $\dot{\delta}_o$. It is likely that q and $\dot{\delta}_o$ will be difficult to measure directly, leaving their determination to micromechanical models of the fracture process.

Figure 3 plots Γ_{ss} as a function of $\hat{\sigma}$ for various crack velocities. The rate exponent for the fracture process was taken to be equal to that of the solid for these simulations, $q = m = 10$. Focusing first on the solid curves with the normalized reference crack opening rate $\dot{\delta}_o/(\dot{\varepsilon}_o\delta_c) = 1$, we note that steady state toughness now *increases* as the crack velocity increases. Within the range of Γ_{ss} shown, the strengthening of the fracture process dominates the hardening in the bulk solid. The two dotted lines on Figure 3 are results for a normalized crack velocity of $\dot{a}/(\dot{\varepsilon}_o R_o) = 100$ and reference crack opening rates of $\dot{\delta}_o/(\dot{\varepsilon}_o\delta_c) = 0.1$ and 10. For a given crack opening rate Eqn. (6) indicates that the traction acting across the crack faces decreases as $\dot{\delta}_o$ increases. Crudely, increasing $\dot{\delta}_o$ is similar to decreasing $\hat{\sigma}$ at a given opening rate.

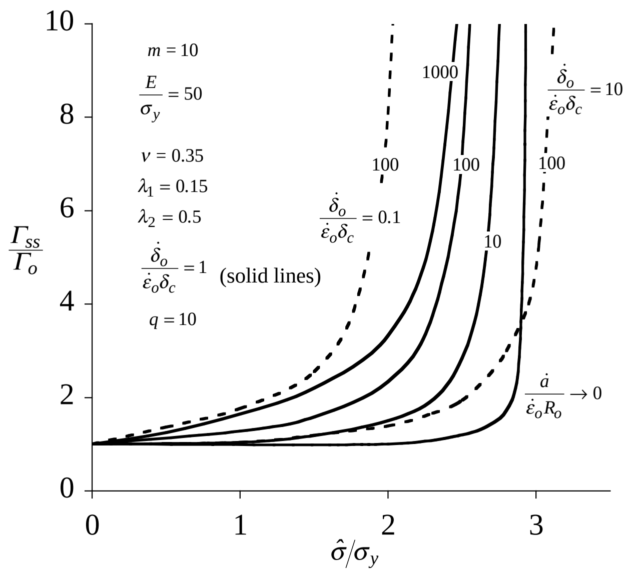

Figure 3: Toughness versus peak cohesive strength for a rate dependent traction-separation law with $q = m = 10$.

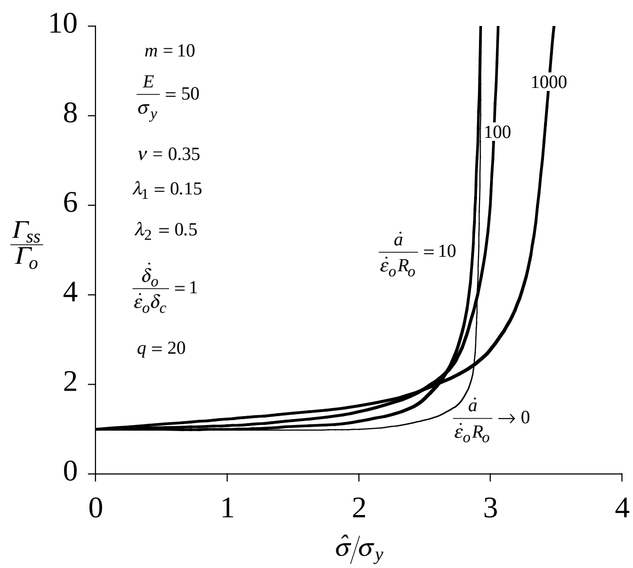

Figure 4: Toughness versus peak cohesive strength for a rate dependent traction-separation law with $q = 2m = 20$.

Notice that the solid curves in Figure 3 seem to approach the $\dot{a}/(\dot{\varepsilon}_o R_o) \to 0$ curve from the left as the crack velocity decreases. This appearance is due to the range of Γ_{ss} shown in the figure. Notice that the $\dot{a}/(\dot{\varepsilon}_o R_o) = 100$, $\dot{\delta}_o/(\dot{\varepsilon}_o \delta_c) = 10$ simulations cross over the $\dot{a}/(\dot{\varepsilon}_o R_o) \to 0$ curve. This is also the case for the $\dot{\delta}_o/(\dot{\varepsilon}_o \delta_c) = 1$ cases, however the crossover occurs at much higher values of Γ_{ss}. A similar change in the toughness versus crack velocity trend is evident for a value of $q = 2m$ to be presented next.

As we have stated throughout q and $\dot{\delta}_o$ could be obtained from a micromechanical analysis. Kramer and Berger [8] present a model for craze widening and under their assumptions the rate exponent for the craze widening is predicted to be twice that for bulk deformations. We note that their assumed form of the bulk constitutive law was power law viscous which is similar to Eqn. (1) except that no yield surface exists, i.e. the additive constant of 1 is removed from the left hand side of (1) and plastic straining occurs at all stress levels. For increasing levels of q Eqn. (6) indicates that for a given applied opening rate the traction acting across the crack surfaces decreases. As shown on Figure 2 the rate independent fracture process limit corresponds to $q \to \infty$. Hence, an increase in q will have similar effects on Γ_{ss} as an increase in $\dot{\delta}_o$. Figure 4 plots Γ_{ss} as a function of $\hat{\sigma}$ for three crack velocities and $q = 2m = 20$. Here again a crossover in the trend of toughness versus velocity occurs. For static peak cohesive stresses lower than approximately $2.7\sigma_y$, Γ_{ss} increases slightly as $\dot{a}$ increases. However, for $\hat{\sigma} > 2.7\sigma_y$ the toughness decreases dramatically as the crack velocity increases (within the range of velocities shown).

4. DISCUSSION

In this work a rate dependent bulk material was coupled with a rate dependent fracture process zone. When the fracture process is rate independent the rate hardening in the bulk solid allows the tractions ahead of the crack tip to elevate and overcome the strength of the cohesive zone. Hence, the toughness of the material decreases as the crack velocity increases. For a rate dependent fracture process zone where both the toughness and strength increase with increasing crack opening rate predictions of the model are more complicated. However, a simple rule of thumb could be proposed: if the peak cohesive stress is less than approximately $3\sigma_y$ then the steady state toughness will increase with increasing crack velocity while the opposite trend holds for $\hat{\sigma} > 3\sigma_y$. The coefficient of 3 is a remnant of the perfectly plastic description of the static stress-strain behavior and the introduction of strain hardening will change the magnitude of the peak stress where this transition occurs. Lastly, the rate of increase/decrease of Γ_{ss} with respect to crack velocity is quite sensitive to the q and $\dot{\delta}_o$ parameters of the fracture process.

REFERENCES

1. Dean, R.H. and Hutchinson, J.W. (1980) *In: Fracture Mechanics: Twelfth Conference*, 383-405.
2. Drugan, W.J., Rice, J.R. and Sham T-L. (1982) *J. Mech. Phys. Solids* 30, 447-473.
3. Marusich, T.D. and Ortiz, M. (1995) *Int. J. Num. Meth. Engng*. 38, 3675-3694.
4. Xia, L., Shih, C.F. (1995) *J. Mech. Phys. Solids*, 43, 1953-1981.
5. Tvergaard, V. and Hutchinson, J.W. (1992) *J. Mech. Phys. Solids*, 40, 1377-1397.
6. Landis, C.M., Pardoen, T. and Hutchinson, J.W. (2000), *Mech. Mater.*, 32, 663-678.
7. Wei, Y. and Hutchinson, J.W. (1997) *J. Mech. Phys. Solids*, 45, 1253-1273.
8. Kramer, J.K. and Berger, L.L. (1990) *Adv. Polym. Sci.*, 91/92, 1-68.